Published in final edited form as:
J Neurochem. 2012 May ; 121(3): 438–450. doi:10.1111/j.1471-4159.2012.07695.x.

Cytosolic acidification and intracellular zinc release in hippocampal neurons

Lech Kiedrowski
The Psychiatric Institute, Departments of Psychiatry and Pharmacology, The University of Illinois at Chicago, Chicago, Illinois 60612, USA

Abstract

In neurons exposed to glutamate, Ca^{2+} influx triggers intracellular Zn^{2+} release via an as yet unclear mechanism. Since glutamate induces a Ca^{2+}-dependent cytosolic acidification, the present work tested the relationships among intracellular Ca^{2+} concentration ($[Ca^{2+}]_i$), intracellular pH (pH_i), and $[Zn^{2+}]_i$. Cultured hippocampal neurons were exposed to glutamate and glycine (Glu/Gly), while $[Zn^{2+}]_i$, $[Ca^{2+}]_i$ and pH_i were monitored using FluoZin-3, Fura2-FF, and 2′,7′-bis-(2-carboxyethyl)-5(6)-carboxyfluorescein, respectively. Glu/Gly applications decreased pH_i to 6.1 and induced intracellular Zn^{2+} release in a Ca^{2+}-dependent manner, as expected. The pH_i drop reduced the affinity of FluoZin-3 and Fura-2-FF for Zn^{2+}. The rate of Glu/Gly-induced $[Zn^{2+}]_i$ increase was not correlated with the rate of $[Ca^{2+}]_i$ increase. Instead, the extent of $[Zn^{2+}]_i$ elevations corresponded well to the rate of pH_i drop. Namely, $[Zn^{2+}]_i$ increased more in more highly acidified neurons. Inhibiting the mechanisms responsible for the Ca^{2+}-dependent pH_i drop (plasmalemmal Ca^{2+} pump and mitochondria) counteracted the Glu/Gly-induced intracellular Zn^{2+} release. Alkaline pH (8.5) suppressed Glu/Gly-induced intracellular Zn^{2+} release whereas acidic pH (6.0) enhanced it. A pH_i drop to 6.0 (without any Ca^{2+} influx or glutamate receptor activation) led to intracellular Zn^{2+} release; the released Zn^{2+} (free Zn^{2+} plus Zn^{2+} bound to Fura-2FF and FluoZin-3) reached 1 μM.

Keywords

Fura-2FF; FluoZin-3; BCECF; TPEN; 2-deoxy-D-glucose; vanadate; rotenone; oligomycin

Introduction

Destabilization of zinc homeostasis has been implicated in the degeneration of ischemic neurons (Koh et al. 1996). Recent data indicate that neurons containing zinc and glutamate in their synaptic vesicles are primarily responsible for extra- and intracellular $[Zn^{2+}]$ ($[Zn^{2+}]_i$) elevations taking place during spreading depression monitored in hippocampal slices (Carter et al. 2011). Similar phenomena may take place during repetitive spreading depression events, such as peri-infarct depolarizations which contribute to neurodegeneration in animal models of stroke (Mies et al. 1993). However, vesicular Zn^{2+} release is not solely responsible for the increases in $[Zn^{2+}]_i$ because elevated Zn^{2+} levels following injury were also observed in thalamic neurons which are not innervated by fibers containing zinc and glutamate in synaptic vesicles (Land and Aizenman 2005) and also in neurons of ZnT3 knockout mice that lack zinc in synaptic vesicles (Lee et al. 2000). In such instances, $[Zn^{2+}]_i$ elevates due to a Zn^{2+} release from intracellular stores. A number of

Correspondence to: Lech Kiedrowski, Ph.D., The Psychiatric Institute, 1601 W. Taylor St., Room 564, Chicago, IL 60612, Phone: 312 413-4559, Fax: 312 413-4569, Lkiedr@psych.uic.edu.

investigators reported a Ca^{2+}-dependent Zn^{2+} release from intracellular stores in glutamate-treated neurons (Sensi et al. 2003; Dineley et al. 2008; Dittmer et al. 2009; Kiedrowski 2011). The mechanism of this Ca^{2+}-dependent Zn^{2+} release remains unclear. Oxidative agents are known to induce Zn^{2+} release from intracellular stores (Aizenman et al. 2000) and Dineley et al. (2008) suggested that intracellular zinc is released in glutamate-treated neurons due to a Ca^{2+}-dependent production of reactive oxygen species. Intracellular pH (pH_i) fluctuations also strongly affect $[Zn^{2+}]_i$ levels following activation of glutamate receptors (Frazzini et al. 2007; Kiedrowski 2011). The present work follows up on the latter findings and tests the idea that glutamate-induced and Ca^{2+}-dependent cytosolic acidification, which is well recognized (Hartley and Dubinsky 1993; Irwin et al. 1994; Koch and Barish 1994; Wang et al. 1994), may serve as a trigger to induce intracellular Zn^{2+} release. The new data support this idea.

Materials and Methods

Primary cultures of mouse hippocampal neurons

A SPOT™ kit from the University of Illinois at Chicago Research Resources Center (http://www.rrc.uic.edu/portal/SPOT_Culture_Kit) was used to prepare primary cultures of hippocampal neurons obtained from c57/bl/6 mice at embryonic day 16. The kit production was approved by the Institutional Animal Care and Use Committee. Cells from a single kit were plated on about 30 glass coverslips, as previously described (Kiedrowski, 2011). The cells were used for experiments after 13 days *in vitro*.

Fluorescence imaging and superfusion equipment

Hoffman modulation contrast images were taken using a Zeiss LD A-Plan 20X/0.3 HMC objective (Carl Zeiss Mikroskopie, Jena, Germany). Fluorescence was monitored using a Zeiss Fluar 20x, NA 0.75 objective and an Attofluor digital imaging system (Atto Instruments, Rockville, MD) connected to Zeiss Axiovert 100 microscope. Superfusion media were delivered directly onto the cells via an 8-channel manifold (MPRE-8, Cell MicroControls, Norfolk, VA) with a computer-controlled flow using an 8-channel valve switch (cFlow8, Cell MicroControls). Cells were superfused at a rate of 0.5 ml/min at 37°C. Temperature was maintained at 37°C using a bipolar temperature controller (TC2BIP, Cell MicroControls).

Monitoring Fura2-FF and FluoZin-3 fluorescence in neurons

Coverslips with SPOT™ cultures were placed in custom-made 50 μl imaging chambers, where the cells were loaded for 5 minutes at 37°C with 0.1 μM FluoZin-3 AM and 0.1 μM Fura-2FF AM added to the medium in which the cells were cultured. Immediately after the loading, the imaging chamber was superfused with Locke's buffer [(in mM) NaCl (157.6), KCl (2.0), $KHCO_3$ (3.6), $MgCl_2$ (1.0), $CaCl_2$ (1.3), HEPES (10), glucose (5), and pH 7.4 adjusted with Tris], which was delivered directly onto the cells via an 8-channel manifold at 37 °C. For time-lapse imaging, cells were exposed every 5 seconds to a sequence of 340, 380, 488 and 356 nm excitation and the images of fluorescence emitted at >520 nm (F340, F380, F488, and F356) were saved on a computer hard-drive for off-line analysis. At the end of each experiment, the maximal Fura-2FF F340/F380 ratio (Rmax) and the maximal FluoZin-3 F488 signal (Fmax) were measured after saturating the indicators *in situ* with Ca^{2+} and Zn^{2+}, respectively. Rmax was determined while the cells were superfused with Locke's buffer supplemented with 10 μM ionomycin, 10 μM TPEN, and 10 mM $CaCl_2$. To measure Fmax, Locke's buffer was supplemented with 20 μM 1-hydroxypyridine-2-thione zinc salt (pyrithione) and 100 μM $ZnCl_2$. In some experiments, the effect of pH_i change on Fmax was tested. In these experiments, the Fmax-testing medium was supplemented with 5 μM gramicidin to accelerate the adjustment of intracellular to extracellular pH and (2-[N-

morpholino]ethanesulfonic acid instead of HEPES was used when pH was 6.0. Unless stated otherwise, the FluoZin-3 data were expressed as a percentage of Fmax to normalize for artifacts associated with uneven loading of the cells with the indicator (Kiedrowski 2011). Fura-2FF data were expressed in terms of a percentage of Rmax to normalize the data from experiments in which absolute F340/F380 ratio values varied due to technical issues (differences in camera gains or neutral density filters). Fura-2FF isosbestic point (F356) fluorescence data were used to assess intracellular Fura-2FF concentrations reached in various cells and to monitor indicator leakage and/or bleaching during experiments. Unhealthy cells showing the Fura-2FF F340/F380 ratio elevated to Rmax under the basal conditions were occasionally observed; such cells were excluded from analysis. In a few cells, the FluoZin-3 Fmax signal could not be effectively measured because it exceeded the dynamic range of the camera; FluoZin-3 and Fura-2FF data from such cells were excluded from analysis. Data from all other neurons (regardless of the pattern of FluoZin-3 or Fura-2FF signal changes) were analyzed and included in figures showing average responses.

Approximation of intracellular Fura-2FF concentrations

Capillaries (20 μm internal diameter; VitroCom, Mountain Lakes, NJ) were filled with various concentrations of Fura-2FF pentapotassium salt dissolved in 100 mM KNO_3, 50 mM PIPES, 10 mM EGTA, pH 7.2. The isosbestic point fluorescence (F356; 356 nm excitation, 515 nm emission) from the capillaries was measured using the Attofluor imaging system with the same optics and camera settings as those used to monitor the Fura-2FF F356 fluorescence emitted from hippocampal neurons. The Fura-2FF concentration in the capillaries that yielded the same F356 as the average F356 measured in 173 Fura-2FF-loaded neurons was taken as an approximation of the intracellular Fura-2FF concentration. It needs to be stressed that the accuracy of this approach is uncertain. Several factors in addition to Fura-2FF concentration affect intracellular F356. Intracellular viscosity is known to enhance fluorescence intensity (Poenie 1990) and may also slightly shift the isosbestic point (Busa 1992). The viscosity effect would enhance F356 fluorescence emitted from cultured neurons. On the other hand, fluorescence from neurons would be lower than that emitted from capillaries because the pathlength through cultured neurons, 5 to 14 μm, is shorter than the internal diameter of the capillaries.

Approximation of intracellular FluoZin-3 concentrations

This was done as described above for Fura-2FF except that the capillaries were filled with various concentrations of FluoZin-3 tetrapotassium salt dissolved in 100 mM KNO_3, 50 mM PIPES, 10 mM EGTA, 10 mM $ZnSO_4$ (10 μM free Zn^{2+}), pH 7.2. Under such conditions, FluoZin-3 is saturated with Zn^{2+} and its fluorescence (F488; 488 nm excitation and 515 nm emission) reflects the concentration of the indicator. The FluoZin-3 concentration in capillaries yielding the F488 value equal to the average Fmax measured in neurons loaded with FluoZin-3 was taken as an approximation of FluoZin-3 concentration in the neurons.

Measuring FluoZin-3 and Fura-2FF apparent zinc K_d at a pH of 7.2 and 6.1

Fluorescence of media supplemented with 10 nM FluoZin-3 tetrapotassium salt or 10 nM Fura-2FF pentapotassium salt and containing free Zn^{2+} concentrations ranging from 0 to 10 μM was measured at 25°C using a PTI QuantaMaster spectrofluorometer (Photon Technology International, Inc., Birmingham, NJ). The media were prepared using 100 mM KNO_3, 50 mM PIPES, 10 mM EGTA and 0 – 10 mM $ZnSO_4$ at the pH of 7.2 or 6.1 (adjusted using KOH). Free Zn^{2+} concentration was calculated using the WEBMAXC STANDARD program (Patton 2009). The fluorescence of FluoZin-3 was excited at 488 nm (F488) and that of Fura-2FF at 346 nm (F346); the emission was measured in both cases at 515 nm. F346 was chosen to excite Fura-2FF because at this weavelength the fluorescence of Fura-2FF-Zn complex reaches maximum (Kiedrowski, 2011). FluoZin-3 data were fitted

to a 2 parameter equation F488 = Fmax × [Zn]/(K_d + [Zn]); Fura-2FF data were fitted to a 3 parameter equation F346 = y0 + Fmax × [Zn]/(K_d + [Zn]), where Fmax is the maximal F488 or F346, K_d is the apparent zinc dissociation constant, and y0 is the F346 at [Zn] = 0. To fit the data, SigmaPlot 10 software (Systat Software Inc., Richmond, CA) was used.

Approximation of the concentrations of released Zn^{2+}

In a cell loaded with Fura-2FF and FluoZin-3, a certain amount of Zn^{2+} binds to Fura-2FF and FluoZin-3. The concentration of released Zn^{2+} ([Zn released]) sensed by the fluorescent indicators can be defined as:

$$[\text{Zn released}]=[Zn^{2+}]_i+[\text{Fura}-2\text{FF}-\text{Zn}]+[\text{FluoZin}-3-\text{Zn}] \quad [1]$$

where $[Zn^{2+}]_i$ is the free Zn^{2+} concentration in the cytosol, [Fura-2FF-Zn] is the concentration of Fura-2FF-Zn complex and [FluoZin-3-Zn] is the concentration of FluoZin-3-Zn complex.

To approximate [Znreleased], [Fura-2FF-Zn] and [FluoZin-3-Zn] were calculated as described below and $[Zn^{2+}]_i$ was calibrated *in situ* using the equation:

$$[Zn^{2+}]_i=K_d\,(F488-Fmin)/(Fmax-F488) \quad [2]$$

where Fmin is the minimal F488 measured after exposing the cells to 10 μM TPEN, Fmax is the maximal F488 measured as described above, and K_d is the apparent zinc dissociation of FluoZin-3 measured at the pH of 6.1.

[Fura-2FF-Zn] and [FluoZin-3-Zn] were calculated as described by Dineley et al. (2002):

$$[\text{dye}-\text{Zn}]=1/2\,([Zn_t]+K_d+[\text{dye}])-1/2\,\sqrt{\{(-[Zn_t]-K_d-[\text{dye}])^2-4\,[Zn_t][\text{dye}]\}} \quad [3]$$

where [dye-Zn] represents intracellular [Fura-2FF-Zn] or [FluoZin-3-Zn], $[Zn_t]$ represents the total $[Zn^{2+}]$, [dye] represents the total intracellular [Fura-2FF] or [FluoZin-3]. [dye-Zn] was calculated separately for Fura-2FF and FluoZin-3 by testing various $[Zn_t]$ values in eq. 3 and selecting the $[Zn_t]$ at which $[Zn_t]$ − [dye-Zn] = $[Zn^{2+}]_i$. To calculate [Zn released], [dye-Zn] values calculated using eq. 3 and $[Zn^{2+}]_i$ calculated using eq. 2 were entered to eq. 1.

Monitoring intracellular pH (pH_i) in neurons

The assay was conducted as described in detail in Kiedrowski (2011) except that in the experiments in which cells were co-loaded with Fura-2FF and BCECF, the loading BCECF-AM concentration was reduced from 1 μM to 5 nM, such that the intracellular BCECF fluorescence observed after 340 and 380 nm excitation was close to background levels (to minimize Fura-2FF signal contamination by BCECF fluorescence). To monitor BCECF fluorescence, the neurons were exposed every 5 seconds to 488 and 440 nm excitation and the images of fluorescence emitted at >520 nm (F488 and F440) were saved on a computer hard-drive for off-line analysis. In selected experiments, F488/F440 ratios were converted to pH_i values based on *in situ* calibration performed at the end of the experiments as described in Kiedrowski (2011).

Experimental media

Glutamate receptors were activated with 100 μM glutamate and 10 μM glycine (Gly/Glu) dissolved in a nominally Mg^{2+}-free Locke's buffer in which NaCl was substituted with a

chloride salt of N-methyl-D-glucamine, as it was shown earlier that Glu/Gly-induced $[Zn^{2+}]_i$ elevations are greatly enhanced under such conditions (Kiedrowski 2011). To remove Ca^{2+} and Zn^{2+} from the buffer, $CaCl_2$ was omitted and 100 μM EGTA was added. To remove Zn^{2+} but not Ca^{2+}, the buffer was supplemented with 1 mM CaEDTA. The latter was added simultaneously with Glu/Gly. Exposure to Glu/Gly plus CaEDTA lasted no longer than 5 – 10 min, which was not long enough to deplete intracellular Zn^{2+} by the extracellular chelator. In fact, the $[Zn^{2+}]_i$ elevations were not affected by CaEDTA (Kiedrowski 2011).

Testing Zn^{2+} chelation by reagents

F488 fluorescence (488 nm excitation, 515 nm emission) of Locke's buffer supplemented with 100 nM FluoZin-3 tetrapotassium was measured at 25°C using a PTI QuantaMaster spectrofluorometer prior to and after adding 10 nM $ZnSO_4$ using a volumetric 50 mM $ZnSO_4$ standard (Fluka, Germany). Then the tested concentration of a reagent (vanadate, rotenone, oligomycin, or 2DG) was added and F488 was measured again. This was followed by adding 100 μM TPEN to chelate Zn^{2+} and measure Fmin. Finally, Fmax was measured after adding 200 μM $ZnSO_4$ to the same cuvette.

Statistical analysis

SigmaStat 3.5 software (Systat Software Inc., Richmond, CA) was used to determine the statistical significance of the data. SigmaPlot 10 software (Systat Software Inc., Richmond, CA) was used to fit the relationship between the rate of Fura-2FF and FluoZin-3 signal increase to a logarithmic equation:

$$F=a^{*}\exp(-0.5^{*}(\ln(x/x0)/b)^{2}) \quad [4]$$

The rates of Fura-2FF and FluoZin-3 signal increase were calculated by linear regression using the linear portion of the data.

Reagents

Fura-2FF AM and Fura-2FF pentapotassium salt was obtained from Teflabs (Austin, TX, USA). Neurobasal medium, B-27 supplement, BCECF AM, FluoZin-3 AM, and FluoZin-3 tetrapotassium salt were from Invitrogen (Carlsbad, CA, USA). All other reagents were from Sigma-Aldrich (St Louis, MO, USA) unless otherwise stated.

Results

The largest and the most rapid $[Ca^{2+}]_i$ elevations are negatively correlated with $[Zn^{2+}]_i$ increases

Fura-2FF and FluoZin-3 fluorescence were simultaneously monitored in primary cultures of hippocampal neurons exposed to 100 μM glutamate and 10 μM glycine (Glu/Gly). To ensure that the fluorescence changes were related to intracellular Zn^{2+} release, extracellular Zn^{2+} was chelated using 1 mM CaEDTA, a plasma membrane-impermeable Zn^{2+} chelator. After FluoZin-3 and/or Fura-2FF signals were elevated by Glu/Gly applications, the impact of 10 μM TPEN, a plasma membrane-permeable Zn^{2+} chelator, was tested on these signals. Experiments were performed under Na^{+}-free conditions, as a recent study established that under such conditions, Glu/Gly-induced $[Zn^{2+}]_i$ elevations are greatly enhanced (Kiedrowski 2011). Fig. 1a shows data from a typical experiment. Consistent with earlier reports (Devinney et al. 2005; Dineley et al. 2008; Kiedrowski 2011), Glu/Gly applications elevated both Fura-2FF and FluoZin-3 signals and a subsequent application of TPEN eliminated the FluoZin-3 signal in all the cells but failed to decrease the Fura-2FF signal in a majority of the cells, indicating that these signals represent $[Zn^{2+}]_i$ and $[Ca^{2+}]_i$ elevations,

respectively. Surprisingly, in neurons showing the most rapid Glu/Gly-induced $[Ca^{2+}]_i$ elevations reaching Fura-2FF-saturating levels, the $[Zn^{2+}]_i$ increases were the smallest (Fig. 1a, blue traces). In neurons with intermediate rates of a $[Ca^{2+}]_i$ increase, the rates of $[Zn^{2+}]_i$ elevations were the highest (Fig. 1 a, red traces) followed by neurons with slower rates of Fura-2FF signal increase (Fig. 1a, green traces). In the latter neurons upon TPEN application, the Fura-2FF signal decreased and remained low or increased after the initial drop (Fig. 1a, arrow), whereas the FluoZin-3 signal dropped to basal or lower levels. This outcome can be interpreted as follows. When $[Ca^{2+}]_i$ and $[Zn^{2+}]_i$ slowly increase (Fig. 1a, green traces), Fura-2FF primarily binds Zn^{2+} because the affinity of the indicator for Zn^{2+} is much higher than that for Ca^{2+} (Hyrc et al. 2000). When TPEN is applied (arrow in Fig. 1a), it strips Zn^{2+} from Fura-2FF. At this point, Fura-2FF begins to bind Ca^{2+} and depending on the amount of ambient cytosolic Ca^{2+}, the Fura-2FF signal may decrease or increase or remain unchanged. The F340/F380 ratio of the Zn^{2+}-saturated Fura-2FF is about 30% of the Ca^{2+}-saturated Fura-2FF (Kiedrowski 2011), which creates a major ambiguity in Fura-2FF signal interpretation. An increase of F340/F380 ratios after TPEN addition most likely means that $[Ca^{2+}]_i$ was high prior to the TPEN addition, but the high $[Ca^{2+}]_i$ could only be detected after the Zn^{2+} that had been bound to Fura-2FF was stripped by TPEN. A F340/F380 ratio reaching 30% of Rmax, may indicate that Fura-2FF is saturated with Zn^{2+} (Kiedrowski 2011), or it may indicate that $[Zn^{2+}]_i$ rests at picomolar levels but $[Ca^{2+}]_i$ is approaching levels close to the Fura-2FF K_d for Ca^{2+}. Simultaneous monitoring of Fura-2FF and FluoZin-3 signals in combination with an eventual TPEN application allows one to identify at which point the Fura-2FF signal exclusively reports $[Ca^{2+}]_i$. However, certain problems, for example whether Zn^{2+} affects the mechanisms of Ca^{2+} homeostasis, cannot be addressed using this method.

For a better clarity, the data from three representative neurons marked A, B, and C, are singled out in Fig. 1b1–b4. Fig. 1b1 shows a Hoffman modulation contrast and a FluoZin-3 Fmax image of the cells. Despite major differences in the patterns of $[Ca^{2+}]_i$ (Fig. 1b2) and $[Zn^{2+}]_i$ (Fig. 1b3) changes in these three neurons, the patterns of the isosbestic point fluorescence (F356) of Fura-2FF were similar (Fig. 1b4), indicating that cells A, B, C were similarly affected by phenomena such as cell swelling or Fura-2FF leakage or bleaching.

Differences in rates of $[Zn^{2+}]_i$ increase among the cells (Fig. 1a, right panel) may result from differences in Fura-2FF or FluoZin-3 concentrations in these cells. For example, slower rates of $[Zn^{2+}]_i$ increases (blue and green FluoZin-3 traces in Fig. 1a) could result from a greater loading of these cells with the indicators. To test whether this is the case, the relative concentrations of Fura-2FF and FluoZin-3 were determined by measuring the F356 (isosbestic point) fluorescence of Fura-2FF, and Fmax of FluoZin-3 in each cell. In Fig. 1c, the rate of $[Zn^{2+}]_i$ increase in 28 neurons is plotted as a function of F356 (an index of Fura-2FF concentration), Fmax (an index of FluoZin-3 concentration), and F356 + Fmax. As can be seen, there is no correlation between the rate of $[Zn^{2+}]_i$ increase and F356, or Fmax, or both, which indicates that the differences in rates of $[Zn^{2+}]_i$ increase among the cells did not result from differences in Fura-2FF or FluoZin-3 concentrations in these cells.

$[Zn^{2+}]_i$ elevations are associated with a drop in pH_i

The Glu/Gly-induced $[Ca^{2+}]_i$ and $[Zn^{2+}]_i$ elevations were both prevented by application of an NMDA channel blocker MK-801 (Fig. 2a), which indicates that they resulted from activation of NMDA receptors. As expected (Sensi et al. 2003; Dineley et al. 2008; Dittmer et al. 2009), Glu/Gly-induced $[Zn^{2+}]_i$ elevations were Ca^{2+}-dependent; no FluoZin-3 or Fura-2FF signal increase was observed when Glu/Gly was applied under Ca^{2+}-free conditions but as soon as Ca^{2+} was added to the medium, both signals increased (Fig. 2b). To relate FluoZin-3 and Fura-2FF signal changes to pH_i changes, pH_i was monitored in an analogous experiment. When hippocampal neurons were exposed to Glu/Gly in the absence

of Ca^{2+}, pH_i dropped from 7.5 ± 0.03 to 6.7 ± 0.08. A further pH_i drop was observed when Ca^{2+} was added (Fig. 2c). Applications of Glu/Gly in the presence of Ca^{2+} led to a pH_i drop to 6.1 ± 0.03 within 5 minutes. The pH_i drop to 6.7 observed when Glu/Gly was applied in the absence of Ca^{2+} (Fig. 2c) was not caused by Glu/Gly but by the lack of Na^+ in the medium in which Glu/Gly was applied; a similar pH_i drop was observed in neurons exposed to a Na^+-free Locke's buffer without Glu/Gly (Fig. 2c, inset). It appears that the pH_i drop from 6.7 to 6.1 triggers an intracellular Zn^{2+} release but the pH_i drop from 7.5 to 6.7 is insufficient to induce this effect. The drop in the BCECF signal was not affected by Zn^{2+} chelation with TPEN; Zn^{2+} influx caused by application of 100 μM $ZnCl_2$ plus 20 μM pyrithione did not prevent BCECF from reporting pH_i changes (Fig. 2d).

Rapid deregulation of Ca^{2+} homeostasis leads to less pronounced intracellular acidification and smaller $[Zn^{2+}]_i$ increases

After plotting the rate of a FluoZin-3 signal increase as the function of Fura-2FF signal increase and fitting the data to equation 4 (for details see Methods), it became evident that the $[Ca^{2+}]_i$ elevations with rates up to 10% of Fura-2FF Rmax x min^{-1} were positively correlated with the rates of $[Zn^{2+}]_i$ elevations. However, in neurons with higher rates of $[Ca^{2+}]_i$ increases, the correlation becomes negative (Fig. 3a).

Since Glu/Gly-induced $[Zn^{2+}]_i$ elevations appear to be associated with a pH_i drop (Fig. 2b,c), an experiment was designed to measure pH_i in neurons showing various rates of $[Ca^{2+}]_i$ increases. In this experiment, Fura-FF and BCECF fluorescence were simultaneously monitored. The data from neurons with the most rapid rates of Fura-2FF signal increase were singled out and compared to the average data from all other neurons in the same field. It was found that the pH_i drop was smallest in the neurons with the fastest rates of $[Ca^{2+}]_i$ increase (Fig. 3b,c).

The idea that neurons showing particularly fast rates of $[Ca^{2+}]_i$ increase but small $[Zn^{2+}]_i$ increases (blue traces in Fig. 1a) may have been less acidified than other neurons was tested further. To this end, neuronal energy reserves were compromised by substituting glucose with 2-deoxy-D-glucose (2DG), a glucose analog that is phosphorylated but not further metabolized. It was expected that Glu/Gly-induced $[Ca^{2+}]_i$ elevations in such neurons would be accelerated (Vergun et al. 2003). As shown in Fig. 4a (green), in the presence of 2DG the rate of Glu/Gly-induced $[Ca^{2+}]_i$ increase was significantly accelerated and this increase was associated with a slower $[Zn^{2+}]_i$ increase (Fig. 4b) and less pronounced intracellular acidification (Fig. 4c).

Two major mechanisms contribute to intracellular acidification induced by Ca^{2+} influx; first, Ca^{2+} entering the cells is extruded back to the extracellular space by a plasmalemmal Ca^{2+} pump that works as an ATP-fueled Ca^{2+}/H^+ exchanger (Trapp et al. 1996; Wu et al. 1999); second, mitochondria, while they accumulate Ca^{2+}, extrude more protons and the cytosol gets acidified while the matrix becomes more alkaline (Wang et al. 1994; Abad et al. 2004). However, the extent to which mitochondria contribute to the Ca^{2+}-dependent pH_i drop vary significantly among neurons (Abad et al. 2004). Therefore, to test the impact of a Ca^{2+}-dependent pH_i drop on $[Zn^{2+}]_i$ increases, both mechanisms of Ca^{2+}-dependent pH_i drop (the plasmalemmal Ca^{2+} pump and mitochondrial Ca^{2+} accumulation) were compromised simultaneously. To inhibit the plasmalemmal Ca^{2+} pump, 1 mM vanadate (Tiffert and Lew 2001) was used, and to prevent Ca^{2+} accumulation in the mitochondria, 2 μM rotenone, an inhibitor of complex I of the respiratory chain, and 3 μg/ml oligomycin, an inhibitor of mitochondrial ATP synthase were applied. Under such conditions, mitochondria promptly depolarize and cannot accumulate Ca^{2+} (Budd and Nicholls 1996a, b). Fig. 5a shows data from an experiment in which vanadate, rotenone, and oligomycin (VRO) were applied two minutes prior to Glu/Gly. Upon VRO addition, $[Ca^{2+}]_i$ began to increase in many neurons

and a subsequent application of Glu/Gly led to a rapid $[Ca^{2+}]_i$ elevation, leading to Fura-2FF saturation at a rate significantly faster than that observed in control cells exposed to Glu/Gly without VRO (Fig. 5a). As shown in Fig 5b, VRO treatment compromised the ability of Glu/Gly to induce an intracellular Zn^{2+} release. As expected, the Glu/Gly-induced cytosolic acidification was significantly reduced when Glu/Gly was applied in the presence of VRO (Fig. 5c).

Alkaline pH counteracts and acidic pH promotes a Glu/Gly-induced intracellular Zn^{2+} release

To further test the role of pH_i decrease in Glu/Gly-induced intracellular Zn^{2+} release, Glu/Gly-induced intracellular acidification was counteracted by increasing the extracellular pH to 8.5. At such an extracellular pH, the Glu/Gly-induced pH_i drop (Fig. 6a) and $[Zn^{2+}]_i$ increases were suppressed (compare Fig. 6b versus 6c). However, when a rapid drop of pH_i to 6.0 was imposed by applying 5 μM gramicidin and simultaneously reducing extracellular pH to 6.0, the FluoZin-3 signal promptly increased (Fig. 6c). This increase represented a Zn^{2+} release from the intracellular stores because it took place while 1 mM CaEDTA was present in the extracellular solution. The FluoZin-3 signal increase was rapidly obliterated when 10 μM TPEN was added to chelate intracellular Zn^{2+} (Fig. 6c).

Increasing extracellular pH to 8.5 not only counteracts the Glu/Gly-induced pH_i drop (Fig. 6a) but also inhibits Ca^{2+} extrusion by the plasmalemmal Ca^{2+} pump and consequently accelerates $[Ca^{2+}]_i$ elevations in glutamate-treated neurons (Khodorov et al. 1995). The faster rate of $[Ca^{2+}]_i$ increases in neurons with an inhibited Ca^{2+} pump and depolarized mitochondria (VRO, Fig. 5a) compared to neurons with an inhibited Ca^{2+} pump but functional mitochondria (pH 8.5, Fig. 6c) emphasizes the impact of the mitochondrial Ca^{2+} sequestration on $[Ca^{2+}]_i$ clearance.

Inhibition of mitochondrial ATP production by rotenone plus oligomycin is expected to accelerate ATP depletion in Glu/Gly-treated neurons. Therefore, one might be concerned that the VRO effect on intracellular Zn^{2+} release shown in Fig. 5b is caused by a greater ATP depletion rather than the smaller pH_i drop (Fig. 5c). Should this be the case, $[Zn^{2+}]_i$ in VRO-treated neurons should not be affected by a pH_i drop. However, as shown in Fig. 6d, an experimental maneuver resulting in a pH_i drop to 6.0 in VRO-treated neurons led to a prompt $[Zn^{2+}]_i$ increase similar to that observed in neurons not treated with VRO (Fig. 6c).

The ability of 2DG, vanadate, rotenone, and/or oligomycin to counteract Glu/Gly-induced $[Zn^{2+}]_i$ elevations (Figs. 4b and 5b) could be an artifact should these agents be able to chelate Zn^{2+}. Using the approach described in Methods, it was found that none of these agents (at the concentrations used in this study) acted as a Zn^{2+} chelator.

A pH_i drop alone induces intracellular Zn^{2+} release

All experiments described thus far were performed under Na^+-free conditions. One may be concerned about the physiological significance of such data. In fact, in the presence of Na^+, in cultured cortical neurons exposed to the pH of 6.0 for 10 min, Sensi et al. (2003) failed to observe any $[Zn^{2+}]_i$ elevations. In cultured cerebellar granule cells, Isaev et al. (2010) did observe $[Zn^{2+}]_i$ elevations under such conditions but the exposures lasted as long as 30 min. To test whether a pH_i drop to 6.0 performed in the presence of Na^+ leads to an intracellular Zn^{2+} release in hippocampal neurons, the neurons were loaded with Fura-2FF and FluoZin-3 and incubated in Locke's buffer containing 158 mM Na^+. The buffer was nominally Ca^{2+}- and Zn^{2+}-free (it contained 100 μM EGTA to chelate Zn^{2+} and Ca^{2+} contamination) and was supplemented with 5 μM gramicidin to accelerate the adjustment of pH_i to the extracellular pH (Kiedrowski 2011). As shown in Fig. 7a, the gramicidin addition *per se* did not affect the

Fura-2FF or FluoZin-3 signal. However, when pH 6.0 was applied three minutes later, both signals promptly increased and, when 10 μM TPEN was added to chelate the intracellular Zn^{2+}, the FluoZin-3 signal dropped to basal levels in 100% of neurons; the Fura-2FF signal dropped in 84% of neurons (104 of 124 neurons; 6 experiments). Since neither Zn^{2+} nor Ca^{2+} was present in the extracellular medium, the data can be interpreted to indicate that the pH_i drop alone (without any Ca^{2+} influx) was sufficient to induce an intracellular Zn^{2+} and Ca^{2+} release, although the latter was overtly apparent in only 16% of neurons.

Fig. 7b shows average FluoZin-3 data from the same experiment that is shown in Fig. 7a. Fig. 7c shows average FluoZin-3 data from an analogous experiment but performed in the absence of gramicidin. As can be seen, the $[Zn^{2+}]_i$ increase observed after applying pH 6.0 in the absence of gramicidin was much smaller than that observed in the presence or gramicidin. At the end of both experiments, it was tested whether the FluoZin-3 Fmax is affected by a pH change from 6.0 to 7.4. To this end, 100 μM $ZnCl_2$, 20 μM pyrithione, and 5 μM gramicindin were applied and during the exposure the pH was changed from 6.0 to 7.4, a maneuver that promptly affects pH_i (Fig. 2d). As can be seen in Fig. 7b,c, the Fmax signal of FluoZin-3 did not change upon the switch from pH 6.0 to 7.4.

The zinc K_d values of FluoZin-3 and Fura-2FF decrease upon a drop in pH

Although the FluoZin-3 Fmax turned out to be insensitive to acidification in the tested range (Fig. 7b,c), the impact of a pH drop on K_d needed to be determined. To this end, Zn-EGTA buffers with a defined $[Zn^{2+}]$ in the 0 – 10 μM range, calculated using the WEBMAXC STANDARD program (Patton 2009), were prepared and the zinc K_d values of FluoZin-3 and Fura-2FF at a pH of 7.2 and 6.1 were characterized *in vitro*. The zinc K_d values of FluoZin-3 at pH 7.2 and 6.1 were found to be 3.4 nM and 36 nM, respectively (Fig. 8a). The observed drop in FluoZin-3 affinity for Zn^{2+} upon acidification does not confirm the earlier assertion that the chelator portion of FluoZin-3 molecule is insensitive to protonation (Gee et al. 2002). The zinc K_d values of Fura-2FF at pH 7.2 and 6.1 were found to be 3.6 nM and 31 nM, respectively (Fig. 8b). The data are consistent with an acidification-induced drop of Fura-2 (and other Ca^{2+} indicators) affinity for Ca^{2+} (Lattanzio and Bartschat 1991).

Approximation of the amount of Zn^{2+} released from intracellular stores

Using eq. 2 and the Zn^{2+} K_d measured at pH 6.1, 36 nM (Fig. 8a), one can estimate that the FluoZin-3 signal increase in the experiment shown in Fig. 7b represents about 16 nM $[Zn^{2+}]_i$. However, the released Zn^{2+} also includes Zn^{2+} bound to FluoZin-3 and Fura-2FF. To calculate the concentration of the FluoZin-3-Zn complex ([FluoZin-3-Zn]), one needs to estimate the concentration of intracellular FluoZin-3 ([FluoZin-3]). Using the approach described in Methods, it was found that an average [FluoZin-3] in hippocampal neurons was about 1.1 μM. From eq. 3 it was calculated that when [FluoZin-3] is 1.1 μM, $[Zn^{2+}]_i$ is 16 nM, and K_d is 36 nM, [FluoZin-3-Zn] is 0.34 μM, meaning that Zn^{2+} is bound to 31% of intracelluar FluoZin-3. Looking at Fig. 7b, one can notice that the F488 value corresponding to 16 nM $[Zn^{2+}]_i$ represents 31% of Fmax, as expected from the eq. 3 calculation. Using an analogous approach for Fura2FF (for details see Methods) it was found that [Fura-2FF] and [Fura-FF-Zn] were about 2.7 μM, and 0.92 μM, respectively. After entering the respective values to eq. 1, one can calculate that [Zn^{2+} released] = 0.016 μM + 0.34 μM + 0.92 μM = 1.276 μM, meaning that the fluorescent Zn^{2+} indicators chelated about 99% of released Zn^{2+}.

The accuracy of the above calculation relies in part on calibrations of intracellular Fura-2FF and Fluo-Zin-3 concentrations which, as explained in Methods, are uncertain. Nevertheless, considering that the cells were loaded with very low concentrations of Fura-2FF AM and FluoZin-3 AM (0.1 μM) and for 5 min only, the approximated intracellular Fura-2FF and

Fluo-Zin-3 concentrations, 2.7 and 1.1 μM, respectively, are about what one would expect from an extrapolation of the data obtained by others (Dineley et al. 2002; Krężel and Maret 2006) who loaded cells with higher concentrations of the dyes and/or for a longer time (20 – 30 min).

Discussion

Earlier work showed that elevated $[Zn^{2+}]_i$ levels in Glu/Gly-treated neurons are promptly cleared from the cytosol in a pH dependent manner – the faster the pH_i increase, the faster the $[Zn^{2+}]_i$ clearance (Kiedrowski 2011). Since activation of Ca^{2+} influx via ionotropic glutamate receptors leads to a pH_i decrease, it is possible that the Glu/Gly-induced pH_i drop promotes intracellular Zn^{2+} release, which was tested in the present experiments.

The new data causally link a Glu/Gly-induced cytosolic acidification with the mechanism of intracellular Zn^{2+} release. In fact, a pH_i drop alone (without any Ca^{2+} influx) is a stimulus sufficient to induce an intracellular Zn^{2+} release in hippocampal neurons (Fig. 7a). Therefore, it appears that the Glu/Gly-induced intracellular Zn^{2+} release in this model depends on a Ca^{2+} influx because the latter is necessary to decrease pH_i to levels low enough (Fig. 2c) to trigger the mechanism of Zn^{2+} release. The pH_i drop must be large enough, well below 6.7, to trigger an intracellular Zn^{2+} release, as smaller pH_i decreases are ineffective (Fig. 2a). In the absence of a protonophore, short lasting applications of low extracellular pH do not decrease pH_i low enough to induce a major intracellular Zn^{2+} release (compare the data in Fig. 7b versus 7c). The reason that Na^+ reduces Glu/Gly-induced intracellular Zn^{2+} release is that it counteracts a pH_i drop (Kiedrowski, 2011). If a pH_i drop to 6.0 is imposed in the presence of Na^+, Zn^{2+} is released from intracellular stores, as expected (Fig. 7a,b).

Since intracellular Zn^{2+} release in this experimental model is triggered by a Ca^{2+} influx (Fig. 2b), it was surprising to notice that neurons showing the fastest rates of $[Ca^{2+}]_i$ increase are the most sluggish in releasing Zn^{2+} from intracellular stores (Fig. 1a, blue traces). These seemingly paradoxical data can be explained in terms of the pH_i decrease being less pronounced in the neurons that increase $[Ca^{2+}]_i$ at the fastest rates (Fig. 3b,c). This conclusion is supported by the finding that neurons with compromised energy reserves behave the same way; they increase $[Ca^{2+}]_i$ faster (Fig. 4a) but acidify less (Fig. 4c) and release less Zn^{2+} from intracellular stores (Fig. 4b) than control neurons. It appears that healthier neurons, which are able to cope with large Ca^{2+} loads for a longer time, acidify more due to the plasmallemal Ca^{2+} pump and mitochondrial activities and therefore release more Zn^{2+} from intracellular stores.

The mechanism of acidification-induced intracellular Zn^{2+} release needs to be further elucidated. Whereas Zn^{2+} may be displaced from metallothioneins and other zinc-binding ligands by protons (Li et al. 1954; Jiang et al. 2000; Sensi et al. 2003), it is unclear whether this process takes place primarily in the cytosol or in zinc-storing organelles or both. While metallothioneins are considered the primary source of Zn^{2+} that could be released upon acidification (Shuttleworth and Weiss 2011), the data of Maret and colleagues (Jiang et al. 2000) suggest that metallothioneins release Zn^{2+} only after pH drops below 5.0. Therefore, the extent to which metallothioneins participate in the here observed intracellular Zn^{2+} release triggered by a pH_i drop to 6.0 (Fig. 7b) remains unclear. One should consider that that a pH_i drop could reverse a H^+/Zn^{2+} exchange in the organelles that use this mechanism to accumulate Zn^{2+} (Colvin 2002; Ohana et al. 2009). Such a reversal would result in a cytosolic $[Zn^{2+}]$ elevation due to the Zn^{2+} efflux from such organelles.

The pathways of intracellular Zn^{2+} release may also include mitochondrial Zn^{2+} fluxes. Dittmer et al. (2009), using cultured hippocampal neurons expressing genetically-encoded Zn^{2+} sensors, observed that glutamate applications lead to a $[Zn^{2+}]$ drop in the mitochondrial matrix and a $[Zn^{2+}]$ increase in the cytosol. Their data indicate that Zn^{2+} is being released from the mitochondria to the cytosol and confirm the earlier conclusions of Sensi et al. (2003). Such glutamate-induced mitochondrial Zn^{2+} fluxes could be strongly affected by a concomitant Ca^{2+}-dependent pH decrease in the cytosol and in the mitochondrial matrix (Bolshakov et al. 2008). However, the extent to which mitochondria represent the intracellular compartments releasing Zn^{2+} in response to cytosolic acidification is not yet clear. Sensi et al. (2003) reported that brief (10 min) exposures of cortical neurons to an extracellular pH of 6.0 do not induce intracellular Zn^{2+} release unless a protonophore, carbonyl cyanide 4-(trifluoromethoxy)phenylhydrazone (FCCP), is applied. They concluded that Zn^{2+} is released from FCCP-depolarized mitochondria and that the resulting $[Zn^{2+}]_i$ elevations are enhanced at a lower pH_i because many Zn^{2+}-buffering mechanisms, including Zn^{2+} binding to metallothioneins, are less effective at acidic pH (Frazzini et al. 2007; Sensi et al. 2009). However, the fact that protonophores, such as FCCP, promote $[Zn^{2+}]_i$ elevations does not necessarily imply that Zn^{2+} is released from the mitochondria. FCCP facilitates proton flux through all biological membranes including acidic organelles that store Zn^{2+}. FCCP application *per se* induces a pH_i drop (Wang et al. 1995; Stout et al. 1998). FCCP applied at an acidic extracellular pH, by accelerating proton influx across the plasma membrane, increases the rate of intracellular acidification. FCCP may induce intracellular Zn^{2+} release by promoting the same acid-sensitive mechanism as gramicidin does (Fig. 7). The role of mitochondria in increasing $[Zn^{2+}]_i$ levels following FCCP application may be that the FCCP-depolarized mitochondria do not accumulate Zn^{2+} (Malaiyandi et al. 2005) that is released from some other intracellular Zn^{2+} stores in response to a pH_i drop.

The mechanisms of Zn^{2+} homeostasis and their sensitivity to acidification may differ among various neurons. For example, an application of pH 6.0 to hippocampal neurons promptly increased $[Zn^{2+}]_i$ (Fig. 7c), whereas this was not observed in cortical neurons (Sensi et al. 2003). In cerebellar granule cells, $[Zn^{2+}]_i$ elevations were observed when the exposures to pH 6.0 were prolonged to 30 min (Isaev et al. 2010). Considering that various neuronal populations in the brain are differently innervated by zinc-containing fibers (Palmiter et al. 1996), one may expect that the mechanisms of Zn^{2+} homeostasis in these neurons quantitatively or qualitatively differ as they evolve to handle different Zn^{2+} levels.

It is interesting to notice that thalamic neurons which do not receive any Zn^{2+}-containing innervation (Palmiter et al. 1996) do show elevated intracellular Zn^{2+} levels after the damage caused by a target loss (Land and Aizenman 2005). Apparently, these neurons release Zn^{2+} from internal stores. Typically, it is speculated that such an intracellular Zn^{2+} release is triggered by oxidative and/or nitrosative stress (Shuttleworth and Weiss 2011). Support for this idea comes from observations that applications of oxidants (Aizenman et al. 2000) or nitric oxide donors (Berendji et al. 1997; Frederickson et al. 2002) induce intracellular Zn^{2+} release. The present data do not question the role of reactive oxygen and nitosative species in inducing intracellular zinc release. However, considering the impact of the pH_i drop on $[Zn^{2+}]_i$ (Fig. 6b,c; 7a,b), the extent to which endogenously produced reactive oxygen/nitrosative species versus pH_i drop mediate intracellular Zn^{2+} release in neurons exposed to ischemic and/or excitotoxic stimuli needs to be determined in future studies.

Ischemic brain tissue acidifies due to ATP hydrolysis (Gault et al. 1994), lactate accumulation (Smith et al. 1986), and insufficient H^+ clearance (Hertz 1981). This pH_i drop may promote an intracellular Zn^{2+} release similar to that seen *in vitro* (Fig. 7b). The present

data suggest that about 99% of the internally released Zn^{2+} was chelated by Fura-2FF and FluoZin-3. However, in neurons not loaded with Zn^{2+}-chelating agents, the released Zn^{2+} is expected to be buffered or cleared from the cytosol by alternative mechanisms. In particular, Zn^{2+} sequestration in the mitochondria may play an important role (Malaiyandi et al. 2005), which may have unfortunate consequences for cell viability. Zn^{2+} was shown to inhibit the bc1 complex of the respiratory chain (Link and von Jagow 1995) and α-ketoglutarate dehydrogenase in the mitochondria (Brown et al. 2000) and to promote mitochondrial permeability transition (Jiang et al. 2001; Bossy-Wetzel et al. 2004). In fact, Isaev et al. (2010) recently linked the acidosis-induced $[Zn^{2+}]_i$ elevations to a mechanism of the acidosis-induced death of cerebellar granule cells, which was reduced when Zn^{2+} was chelated by TPEN. Considering that preischemic hyperglycemia exacerbates pH_i drop during ischemia (Siemkowicz and Hansen 1981; Smith et al. 1986) and increases ischemic brain damage (Myers and Yamaguchi 1977; Siemkowicz and Hansen 1978), one may speculate that an enhanced intracellular zinc release plays a role in the ischemic vulnerability of hyperglycemic animals.

Acknowledgments

This work was supported by National Institutes of Health Grants 1R21 NS065305 and 5RO3 NS077095 and American Heart Association Grant-in-Aid 0855825G and was presented on poster 450.03 at the 2011 Society for Neuroscience Meeting. The author is grateful to Dr. C. William Shuttleworth for his critical reading of the manuscript, to Dr. John A. Connor for advice on intracellular [Fura-2FF] calibration, and to Dr. Peter G.W. Gettins for access to PTI QuantaMaster spectrofluorometer. The author declares his involvement in SPOT™ culture kit production at the University of Illinois at Chicago Research Resources Center.

Abbreviations used

BCECF	2′,7′-bis-(2-carboxyethyl)-5(6)-carboxyfluorescein
$[Ca^{2+}]_i$ and $[Zn^{2+}]_i$	intracellular Ca^{2+} and Zn^{2+} concentration
CaEDTA	calcium EDTA
2DG	2-deoxy-D-glucose
Fmax	maximal F488
[FluoZin-3-Zn]	concentration of FluoZin-3-Zn complex
[Fura-2FF-Zn]	concentration of Fura-2FF-Zn complex
Glu/Gly	cell exposure to 100 μM glutamate plus 10 μM glycine
pH_i	intracellular pH
pyrithione	1-hydroxypyridine-2-thione zinc salt
Rmax	maximal F340/F380 ratio
TPEN	N,N,N′,N′-tetrakis(2-pyridylmethyl)ethylenediamine
VRO	vanadate + rotenone + oligomycin

References

Abad MF, Di Benedetto G, Magalhaes PJ, Filippin L, Pozzan T. Mitochondrial pH monitored by a new engineered green fluorescent protein mutant. J Biol Chem. 2004; 279:11521–11529. [PubMed: 14701849]

Aizenman E, Stout AK, Hartnett KA, Dineley KE, McLaughlin B, Reynolds IJ. Induction of neuronal apoptosis by thiol oxidation: putative role of intracellular zinc release. J Neurochem. 2000; 75:1878–1888. [PubMed: 11032877]

Berendji D, Kolb-Bachofen V, Meyer KL, Grapenthin O, Weber H, Wahn V, Kroncke KD. Nitric oxide mediates intracytoplasmic and intranuclear zinc release. FEBS Lett. 1997; 405:37–41. [PubMed: 9094420]

Bolshakov AP, Mikhailova MM, Szabadkai G, Pinelis VG, Brustovetsky N, Rizzuto R, Khodorov BI. Measurements of mitochondrial pH in cultured cortical neurons clarify contribution of mitochondrial pore to the mechanism of glutamate-induced delayed Ca^{2+} deregulation. Cell Calcium. 2008; 43:602–614. [PubMed: 18037484]

Bossy-Wetzel E, Talantova MV, Lee WD, Scholzke MN, Harrop A, Mathews E, Gotz T, Han J, Ellisman MH, Perkins GA, Lipton SA. Crosstalk between nitric oxide and zinc pathways to neuronal cell death involving mitochondrial dysfunction and p38-activated K^+ channels. Neuron. 2004; 41:351–365. [PubMed: 14766175]

Brown AM, Kristal BS, Effron MS, Shestopalov AI, Ullucci PA, Sheu KF, Blass JP, Cooper AJ. Zn^{2+} inhibits alpha-ketoglutarate-stimulated mitochondrial respiration and the isolated alpha-ketoglutarate dehydrogenase complex. J Biol Chem. 2000; 275:13441–13447. [PubMed: 10788456]

Budd SL, Nicholls DG. A reevaluation of the role of mitochondria in neuronal Ca^{2+} homeostasis. J Neurochem. 1996a; 66:403–411. [PubMed: 8522981]

Budd SL, Nicholls DG. Mitochondria, calcium regulation, and acute glutamate excitotoxicity in cultured cerebellar granule cells. J Neurochem. 1996b; 67:2282–2291. [PubMed: 8931459]

Busa WB. Spectral characterization of the effect of viscosity on Fura-2 fluorescence: excitation wavelength optimization abolishes the viscosity artifact. Cell Calcium. 1992; 13:313–319. [PubMed: 1623501]

Carter RE, Aiba I, Dietz RM, Sheline CT, Shuttleworth CW. Spreading depression and related events are significant sources of neuronal Zn^{2+} release and accumulation. J Cereb Blood Flow Metab. 2011; 31:1073–1084. [PubMed: 20978516]

Colvin RA. pH dependence and compartmentalization of zinc transported across plasma membrane of rat cortical neurons. Am J Physiol Cell Physiol. 2002; 282:C317–329. [PubMed: 11788343]

Devinney MJ 2nd, Reynolds IJ, Dineley KE. Simultaneous detection of intracellular free calcium and zinc using fura-2FF and FluoZin-3. Cell Calcium. 2005; 37:225–232. [PubMed: 15670869]

Dineley KE, Malaiyandi LM, Reynolds IJ. A reevaluation of neuronal zinc measurements: artifacts associated with high intracellular dye concentration. Mol Pharmacol. 2002; 62:618–627. [PubMed: 12181438]

Dineley KE, Devinney MJ 2nd, Zeak JA, Rintoul GL, Reynolds IJ. Glutamate mobilizes $[Zn^{2+}]$ through Ca^{2+}-dependent reactive oxygen species accumulation. J Neurochem. 2008; 106:2184–2193. [PubMed: 18624907]

Dittmer PJ, Miranda JG, Gorski JA, Palmer AE. Genetically encoded sensors to elucidate spatial distribution of cellular zinc. J Biol Chem. 2009; 284:16289–16297. [PubMed: 19363034]

Frazzini V, Rapposelli IG, Corona C, Rockabrand E, Canzoniero LM, Sensi SL. Mild acidosis enhances AMPA receptor-mediated intracellular zinc mobilization in cortical neurons. Mol Med. 2007; 13:356–361. [PubMed: 17622309]

Frederickson CJ, Cuajungco MP, LaBuda CJ, Suh SW. Nitric oxide causes apparent release of zinc from presynaptic boutons. Neuroscience. 2002a; 115:471–474. [PubMed: 12421613]

Gault LM, Lin CW, Lamanna JC, Lust WD. Changes in energy metabolites, cGMP and intracellular pH during cortical spreading depression. Brain Res. 1994; 641:176–180. [PubMed: 8019846]

Gee KR, Zhou ZL, Qian WJ, Kennedy R. Detection and imaging of zinc secretion from pancreatic beta-cells using a new fluorescent zinc indicator. J Am Chem Soc. 2002; 124:776–778. [PubMed: 11817952]

Hartley Z, Dubinsky JM. Changes in intracellular pH associated with glutamate excitotoxicity. J Neurosci. 1993; 13:4690–4699. [PubMed: 7901350]

Hertz L. Features of astrocytic function apparently involved in the response of central nervous tissue to ischemia-hypoxia. J Cereb Blood Flow Metab. 1981; 1:143–153. [PubMed: 6120175]

Hyrc KL, Bownik JM, Goldberg MP. Ionic selectivity of low-affinity ratiometric calcium indicators: mag-Fura-2, Fura-2FF and BTC. Cell Calcium. 2000; 27:75–86. [PubMed: 10756974]

Irwin RP, Lin S-Z, Long RT, Paul SM. N-methyl-D-aspartate induces a rapid, reversible, and calcium dependent intracellular acidosis in cultured fetal rat hippocampal neurons. J Neurosci. 1994; 14:1352–1357. [PubMed: 8120630]

Isaev NK, Stelmashook EV, Lukin SV, Freyer D, Mergenthaler P, Zorov DB. Acidosis-induced zinc-dependent death of cultured cerebellar granule neurons. Cell Mol Neurobiol. 2010; 30:877–883. [PubMed: 20373017]

Jiang D, Sullivan PG, Sensi SL, Steward O, Weiss JH. Zn^{2+} induces permeability transition pore opening and release of pro-apoptotic peptides from neuronal mitochondria. J Biol Chem. 2001; 276:47524–47529. [PubMed: 11595748]

Jiang LJ, Vasak M, Vallee BL, Maret W. Zinc transfer potentials of the alpha - and beta-clusters of metallothionein are affected by domain interactions in the whole molecule. Proc Natl Acad Sci U S A. 2000; 97:2503–2508. [PubMed: 10716985]

Khodorov B, Pinelis V, Vergun O, Storozhevykh T, Fajuk D, Vinskaya N, Arsenjeva E, Khaspekov L, Lyzin A, Isayev N, Andreeva N, Victorov I. Dramatic effects of external alkalinity on neuronal calcium recovery following a short-duration glutamate challenge: the role of the plasma membrane Ca^{2+}/H^{+} pump. FEBS Lett. 1995; 371:249–252. [PubMed: 7556602]

Kiedrowski L. Cytosolic zinc release and clearance in hippocampal neurons exposed to glutamate - the role of pH and sodium. J Neurochem. 2011; 117:231–243. [PubMed: 21255017]

Koch RA, Barish ME. Perturbation of intracellular calcium and hydrogen ion regulation in cultured mouse hippocampal neurons by reduction of the sodium ion concentration gradient. J Neurosci. 1994; 14:2585–2593. [PubMed: 7910200]

Koh J-Y, Suh SW, Gwag BJ, He YY, Hsu CY, Choi DW. The role of zinc in selective neuronal death after transient global cerebral ischemia. Science. 1996; 272:1013–1016. [PubMed: 8638123]

Krężel A, Maret W. Zinc-buffering capacity of a eukaryotic cell at physiological pZn. J Biol Inorg Chem. 2006; 11:1049–1062. [PubMed: 16924557]

Land PW, Aizenman E. Zinc accumulation after target loss: an early event in retrograde degeneration of thalamic neurons. Eur J Neurosci. 2005; 21:647–657. [PubMed: 15733083]

Lattanzio FA, Bartschat DK. The effect of pH on rate constants, ion selectivity and thermodynamic properties of fluorescent calcium and magnesium indicators. Biochem Biophys Res Commun. 1991; 177:184–191. [PubMed: 2043105]

Lee JY, Cole TB, Palmiter RD, Koh JY. Accumulation of zinc in degenerating hippocampal neurons of ZnT3-null mice after seizures: evidence against synaptic vesicle origin. J Neurosci. 2000; 20:RC79. [PubMed: 10807937]

Li NC, Gawron O, Bascuas G. Stability of Zinc Complexes with Glutathione and Oxidized Glutathione. J Am Chem Soc. 1954:225–229.

Link TA, von Jagow G. Zinc ions inhibit the QP center of bovine heart mitochondrial bc1 complex by blocking a protonatable group. J Biol Chem. 1995; 270:25001–25006. [PubMed: 7559629]

Malaiyandi LM, Vergun O, Dineley KE, Reynolds IJ. Direct visualization of mitochondrial zinc accumulation reveals uniporter-dependent and -independent transport mechanisms. J Neurochem. 2005; 93:1242–1250. [PubMed: 15934944]

Mies G, Iijima T, Hossmann KA. Correlation between peri-infarct DC shifts and ischaemic neuronal damage in rat. Neuroreport. 1993; 4:709–711. [PubMed: 8347812]

Myers RE, Yamaguchi S. Nervous system effects of cardiac arrest in monkeys. Preservation of vision. Arch Neurol. 1977; 34:65–74. [PubMed: 402127]

Ohana E, Hoch E, Keasar C, Kambe T, Yifrach O, Hershfinkel M, Sekler I. Identification of the Zn^{2+} binding site and mode of operation of a mammalian Zn^{2+} transporter. J Biol Chem. 2009; 284:17677–17686. [PubMed: 19366695]

Palmiter RD, Cole TB, Quaife CJ, Findley SD. ZnT-3, a putative transporter of zinc into synaptic vesicles. Proc Natl Acad Sci U S A. 1996; 93:14934–14939. [PubMed: 8962159]

Patton, CW. WEBMAXC STANDARD. 2009. http://www.stanford.edu/~cpatton/webmaxc/webmaxcS.htm

Poenie M. Alteration of intracellular Fura-2 fluorescence by viscosity: a simple correction. Cell Calcium. 1990; 11:85–91. [PubMed: 2354506]

Sensi SL, Paoletti P, Bush AI, Sekler I. Zinc in the physiology and pathology of the CNS. Nat Rev Neurosci. 2009; 10:780–791. [PubMed: 19826435]

Sensi SL, Ton-That D, Sullivan PG, Jonas EA, Gee KR, Kaczmarek LK, Weiss JH. Modulation of mitochondrial function by endogenous Zn^{2+} pools. Proc Natl Acad Sci U S A. 2003; 100:6157–6162. [PubMed: 12724524]

Shuttleworth CW, Weiss JH. Zinc: new clues to diverse roles in brain ischemia. Trends Pharmacol Sci. 2011; 32:480–486. [PubMed: 21621864]

Siemkowicz E, Hansen AJ. Clinical restitution following cerebral ischemia in hypo-, normo- and hyperglycemic rats. Acta Neurol Scand. 1978; 58:1–8. [PubMed: 30250]

Siemkowicz E, Hansen AJ. Brain extracellular ion composition and EEG activity following 10 minutes ischemia in normo- and hyperglycemic rats. Stroke. 1981; 12:236–240. [PubMed: 7233472]

Smith ML, von Hanwehr R, Siesjo BK. Changes in extra- and intracellular pH in the brain during and following ischemia in hyperglycemic and in moderately hypoglycemic rats. J Cereb Blood Flow Metab. 1986; 6:574–583. [PubMed: 3760041]

Stout AK, Raphael HM, Kanterewicz BI, Klann E, Reynolds IJ. Glutamate-induced neuronal death requires mitochondrial calcium uptake. Nature Neuroscience. 1998; 1:366–373.

Tiffert T, Lew VL. Kinetics of inhibition of the plasma membrane calcium pump by vanadate in intact human red cells. Cell Calcium. 2001; 30:337–342. [PubMed: 11733940]

Trapp S, Lueckermann M, Kaila K, Ballanyi K. Acidosis of hippocampal neurones mediated by a plasmalemmal Ca^{2+}/H^{+} pump. Neuroreport. 1996; 7:2000–2004. [PubMed: 8905712]

Vergun O, Han YY, Reynolds IJ. Glucose deprivation produces a prolonged increase in sensitivity to glutamate in cultured rat cortical neurons. Exp Neurol. 2003; 183:682–694. [PubMed: 14552910]

Wang GJ, Randall RD, Thayer SA. Glutamate-induced intracellular acidification of cultured hippocampal neurons demonstrates altered energy metabolism resulting from Ca^{2+} loads. J Neurophysiol. 1994; 72:2563–2569. [PubMed: 7897473]

Wang GJ, Richardson SR, Thayer SA. Intracellular acidification is not a prerequisite for glutamate-triggered death of cultured hippocampal neurons. Neurosci Lett. 1995; 186:139–144. [PubMed: 7777183]

Wu ML, Chen JH, Chen WH, Chen YJ, Chu KC. Novel role of the Ca^{2+}-ATPase in NMDA-induced intracellular acidification. Am J Physiol. 1999; 277:C717–727. [PubMed: 10516102]

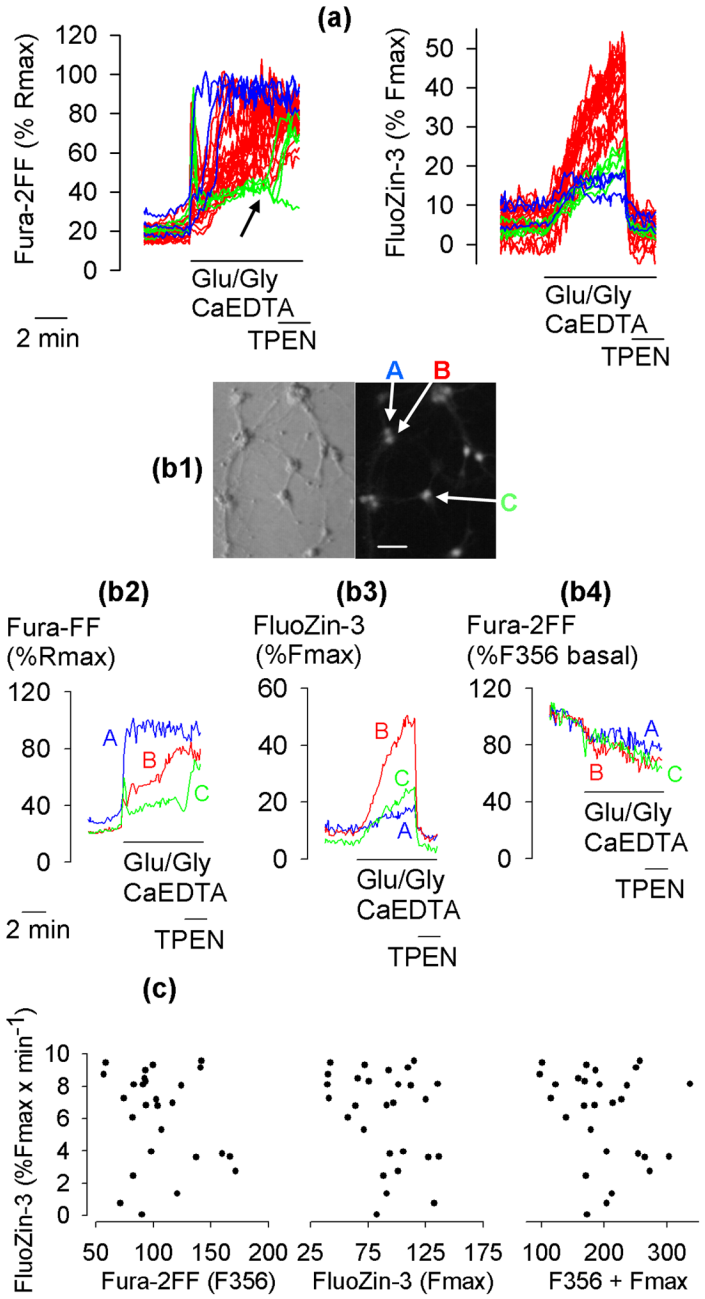

Figure 1.

The relationship between the rates of $[Ca^{2+}]_i$ and $[Zn^{2+}]_i$ increases. (a) Simultaneously monitored Fura-2FF and FluoZin-3 signals in 28 hippocampal neurons exposed to 100 μM glutamate and 10 μM glycine (Glu/Gly) under Na^+-free conditions (Na^+ was removed at the time Glu/Gly was added) with Na^+ substituted with N-methyl-D-glucamine. Extracellular Zn^{2+} was chelated using 1 mM CaEDTA. Where indicated, 10 μM TPEN was added to chelate intracellular Zn^{2+}. The colors, blue, red, and green, identify neurons with high, intermediate, and slow rates of Fura-2FF signal increase, respectively. (b1–b4) Data from three exemplar neurons A, B, and C from the population of 28 neurons shown in panel (a). (b1) A Hoffman modulation contrast image (left) and a FluoZin-3 Fmax image (right) of the

neurons. Bar = 50 μm. (b2, b3) Fura-2FF and FluoZin-3 signals expressed as a percentage of Rmax and Fmax signal, respectively. The Rmax and Fmax signals were measured at the end of the experiment (not shown) as described in Methods. (b4) Fura-2FF F356 signal (isosbestic point) expressed as a percentage of F356 signal measured prior to Glu/Gly application. (c) The rate of FluoZin-3 signal increase does not correlate with the Fura-2FF isosbestic point (F356) fluorescence (left), the maximal FluoZin-3 signal (Fmax) (middle), or the sum of F356 and Fmax (right). The data in (a), (b1–b4) and (c) are from the same experiment, which was repeated 5 times with similar results.

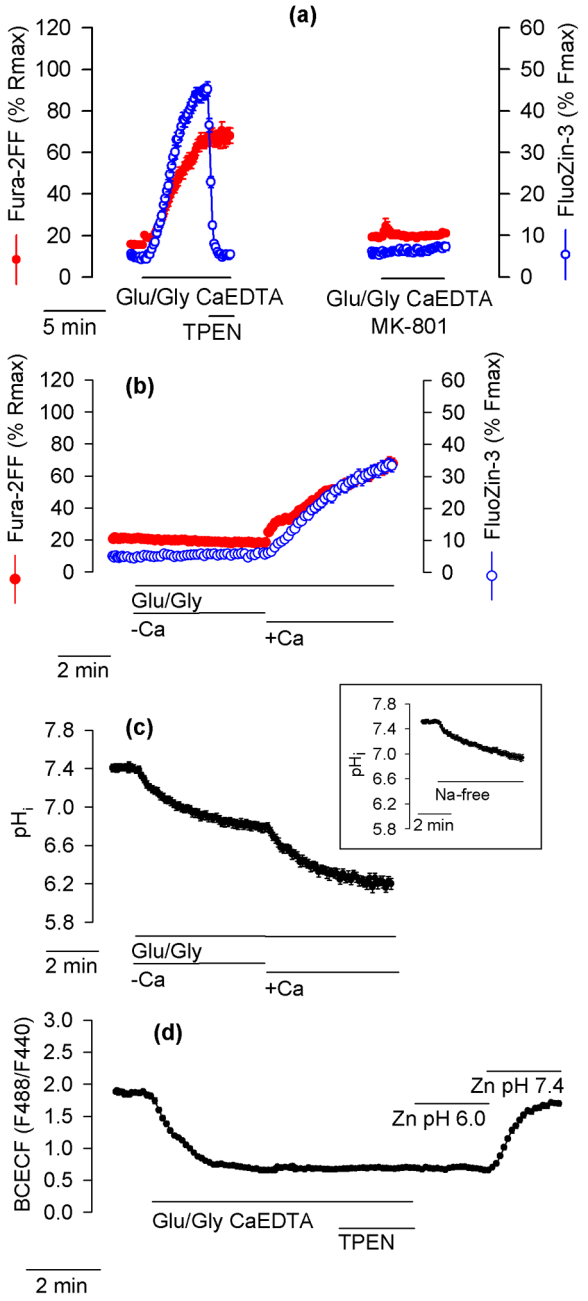

Figure 2.

Glutamate-induced and Ca^{2+}-dependent $[Zn^{2+}]_i$ elevations depend on activation of NMDA receptors and are associated with a drop in pH_i. (a) Blocking NMDA channels with 10 μM MK-801 prevents the Glu/Gly-induced increase of Fura-2FF and FluoZin-3 signal. The data are averages ± SE from 29 (right) and 22 (left) neurons. The experiments were repeated 5 times with similar results. In these and all other experiments, Glu/Gly was applied under Na^+-free conditions (Na^+ was removed at the same time Glu/Gly was added). (b) In the absence of Ca^{2+} (−Ca), Glu/Gly application failed to increase Fura-2FF and FluoZin-3 signals. Only after 1.3 mM $CaCl_2$ was added (+Ca) did both signals increase. (c) Glu/Gly application decreased pH_i in a Ca^{2+}-dependent manner. The cells were exposed to Glu/Gly

under analogous experimental conditions as in (b). Note that the Ca^{2+}-dependent FluoZin-3 and Fura-2FF signal increase shown in (b) is associated with a Ca^{2+}-dependent pH_i drop. The initial pH_i drop, observed in the absence of Ca^{2+} (−Ca), is caused not by Glu/Gly but by removal of Na^+. As shown in the inset, an analogous pH_i drop is observed when Na^+-free Locke's buffer (without Glu/Gly) is applied. The data are averages ± SE from 28 (b), 11 (c) and 14 (inset) neurons monitored in a single experiment. All experiments were repeated 4 – 5 times with similar results. (d) Zn^{2+} chelation with 10 μM TPEN does not affect the Glu/Gly-induced drop in the intracellular BCECF signal. At the end of the experiment, Zn^{2+} influx and pH_i changes were imposed by an application of 100 μM $ZnCl_2$, 20 μM pyrithione, and 5 μM gramicidin at a pH of 6.0 (Zn pH 6.0) and a pH of 7.4 (Zn pH 7.4), as indicated. The data are averages ± SE from 31 neurons monitored in a single experiment that was repeated 3 times with similar results.

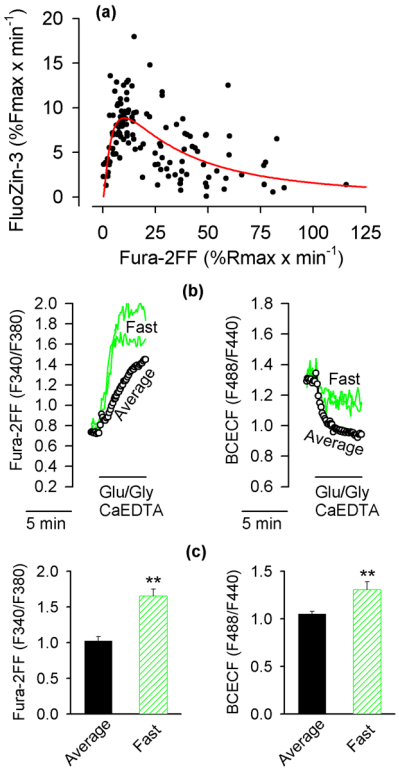

Figure 3.

The neurons with the fastest rates of $[Ca^{2+}]_i$ increase acidify less and release less Zn^{2+} from intracellular stores. (a) The relationship between the rate of Fura-2FF signal increases and the rate FluoZin-3 signal increases. The data are from 128 individual neurons monitored in 6 experiments analogous to the one shown in Fig. 1a. The red line indicates the closest fit of the data to equation 4. Note that the rate on FluoZin-3 signal increase is positively correlated with the rate of Fura-2FF signal increase only up to about 10% of Rmax x min^{-1}. At faster rates of Fura-2FF signal increases, the correlation becomes negative. (b) The neurons with the fastest rates of Fura-2FF signal increases acidify less than other neurons. Intracellular Fura-2FF and BCECF signals were simultaneously monitored in neurons exposed to Glu/Gly under the experimental conditions identical to those described in Fig. 1a. The neurons with the fastest rate of Fura-2FF signal increases were singled out (Fast; green traces); the data from all other neurons were averaged (Average, black open circles). Note that the neurons with the fastest rate of Fura-2FF signal increases (left panel) show a less pronounced drop in the BCECF signal (right panel). (c) Fura-2FF and BCECF signals measured 5 min after the onset of Glu/Gly application. The data are means ± SE from 4 experiments analogous to the one shown in (b). ** $P < 0.01$, Mann-Whitney Rank Sum Test.

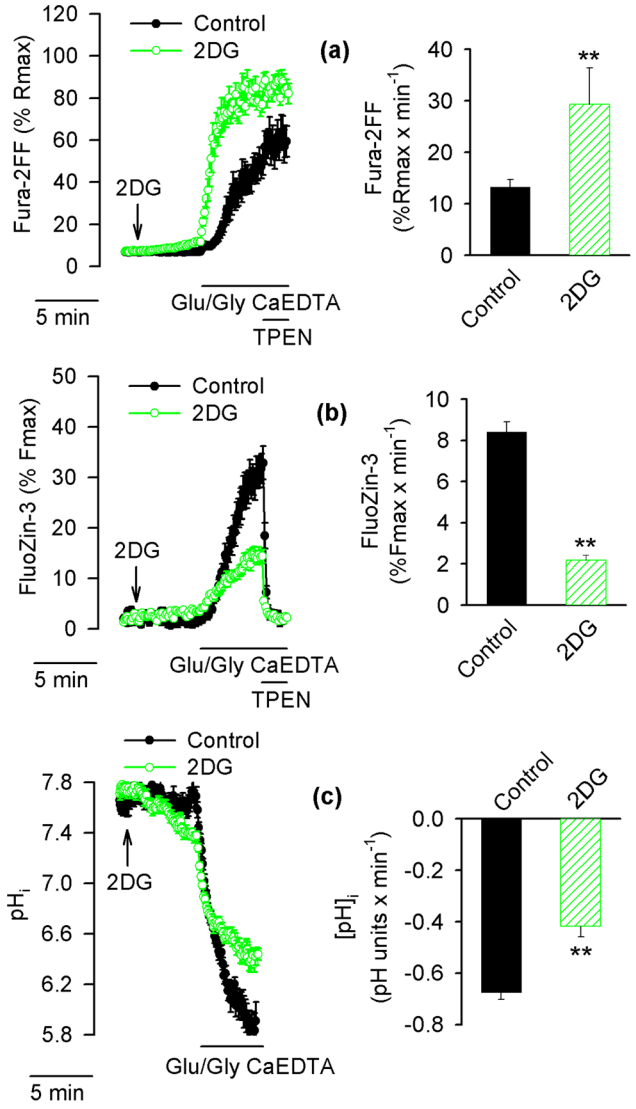

Figure 4.

Effects of substitution of glucose with 2-deoxy-D-glucose (2DG) on $[Ca^{2+}]_i$, $[Zn^{2+}]_i$ and pH_i in Glu/Gly-treated neurons. Fura-2FF- and FluoZin-3-loaded neurons (a and b) or BCECF-loaded neurons (c) were exposed to Glu/Gly as described in Fig. 1 in the presence of glucose (black traces, filled symbols, black bars) or with glucose substituted with 2DG (green traces, open symbols, hatched bars). The arrow indicates when glucose was replaced by 2DG. The data in the left hand panels are averages ± SE from 13 – 22 neurons monitored in a single experiment; the averages ± SE from 4 such experiments are shown in the right hand panel. ** $p < 0.01$ (Student's t-test).

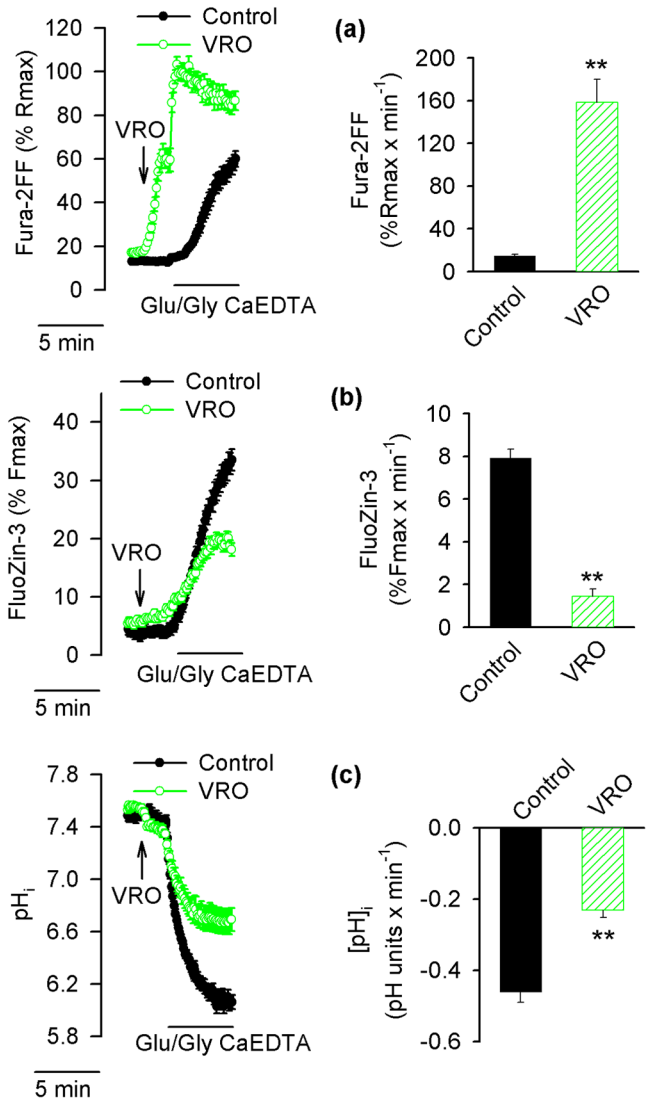

Figure 5.

Effects of vanadate, rotenone, and oligomycin (VRO) on $[Ca^{2+}]_i$, $[Zn^{2+}]_i$ and pH_i in Glu/Gly-treated neurons. Fura-2FF- and FluoZin-3-loaded neurons (a and b) or BCECF-loaded neurons (c) neurons were exposed to Glu/Gly in the presence of 1 mM vanadate (to inhibit the plasmalemmal Ca^{2+} pump) and 2 μM rotenone plus 3 μg/ml oligomycin (to depolarize mitochondria). The arrow indicates when VRO was added. The data in the left hand panels are averages ± SE from 21–31 neurons monitored in a single experiment; the averages ± SE from 5 such experiments are shown in the right hand panel. Black traces, filled symbols, and black bars show data from control neurons. Green traces, open symbols, and hatched bars show data from VRO-treated neurons. ** $p < 0.01$ (Student's t-test).

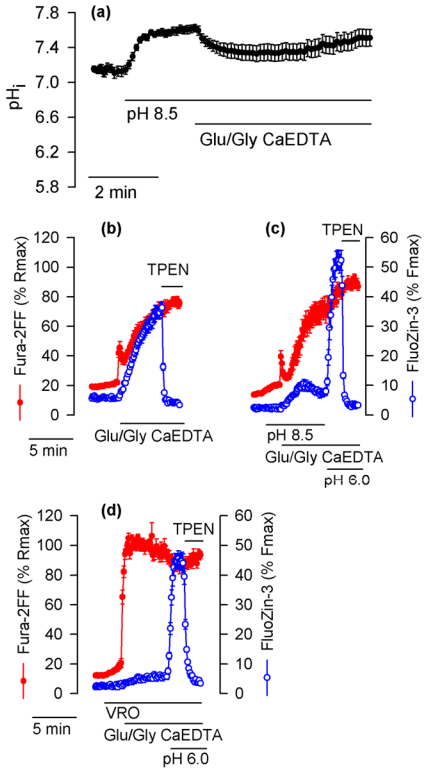

Figure 6.

Alkaline pH inhibits and acidic pH promotes intracellular Zn^{2+} release in Glu/Gly-treated neurons. (a) The effect of alkaline pH on pH_i in cultured hippocampal neurons exposed to Glu/Gly in the presence of 1 mM CaEDTA. The experiment was conducted as those shown in Figs. 4c and 5c (control, black traces) except that where indicated extracelluar pH was increased from 7.4 to 8.5. (b) Fura-2FF and FluoZin-3 signals monitored in a control experiment performed at a pH of 7.4. (c) Analogous experiments with Glu/Gly applied at the pH of 8.5 followed by application of a pH of 6.0. To ensure a prompt drop of pH_i to 6.0, 5 μM gramicidin was applied at the time the extracellular pH was switched form 8.5 to 6.0. Where indicated, 10 μM TPEN was added to chelate Zn^{2+}. (d) Similar experiment to the one shown in (c) but performed in the presence of VRO. The data are averages ± SE from 16 (a), 28 (b), 17 (c), and 22 (d) neurons monitored in a single experiment. All experiments were repeated with similar results 4 – 5 times.

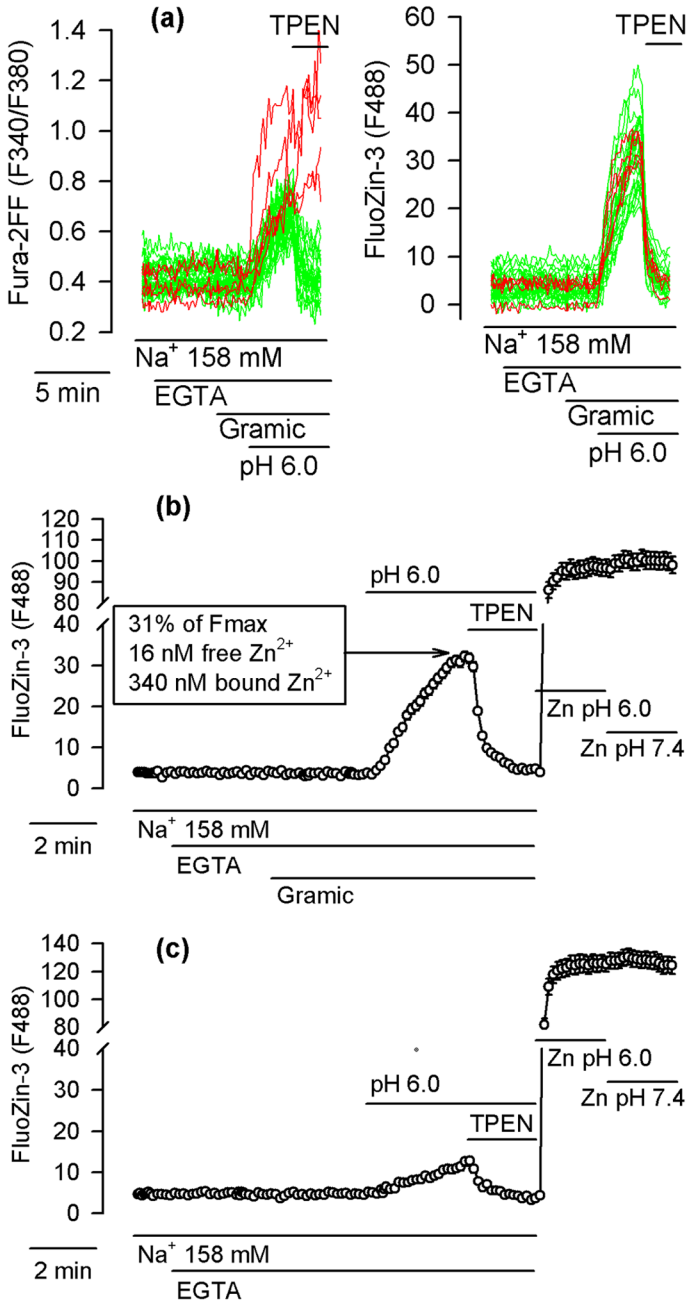

Figure 7.

A pH_i drop (without Ca^{2+} influx) suffices to induce intracellular Zn^{2+} release. (a) Fura-2FF- and FluoZin-3-loaded neurons incubated in a Ca^{2+}-free and Zn^{2+}-free Locke's buffer containing 158 mM Na^+ and supplemented with 100 μM EGTA (EGTA). Where indicated, 5 μM gramicidin (Gramic) was applied to permeabilize the plasma membrane to H^+, Na^+ and K^+; to induce pH_i drop, extracellular pH was decreased to 6.0; TPEN (10 μM) was added to chelate Zn^{2+}. Left and right panels show Fura-2FF and FluoZin-3 data, respectively, simultaneously monitored in 32 neurons. In three neurons (red) unlike in other neurons (green), the Fura-2FF signal failed to drop upon TPEN application. (b) Average FluoZin-3 ± SE data from all cells shown in (a). At the end of this experiment, the maximal

FluoZin-3 signal (Fmax) was measured at a pH of 6.0 (Zn pH 6.0) and a pH of 7.4 (Zn pH 7.4). Note that the pH change failed to affect Fmax. The values listed in the box are discussed in the text. (c) Analogous experiment to the one shown in (b) but without gramicidin. The data are averages ± SE from 24 neurons monitored in a single experiment. All experiments were repeated 5 times with similar results.

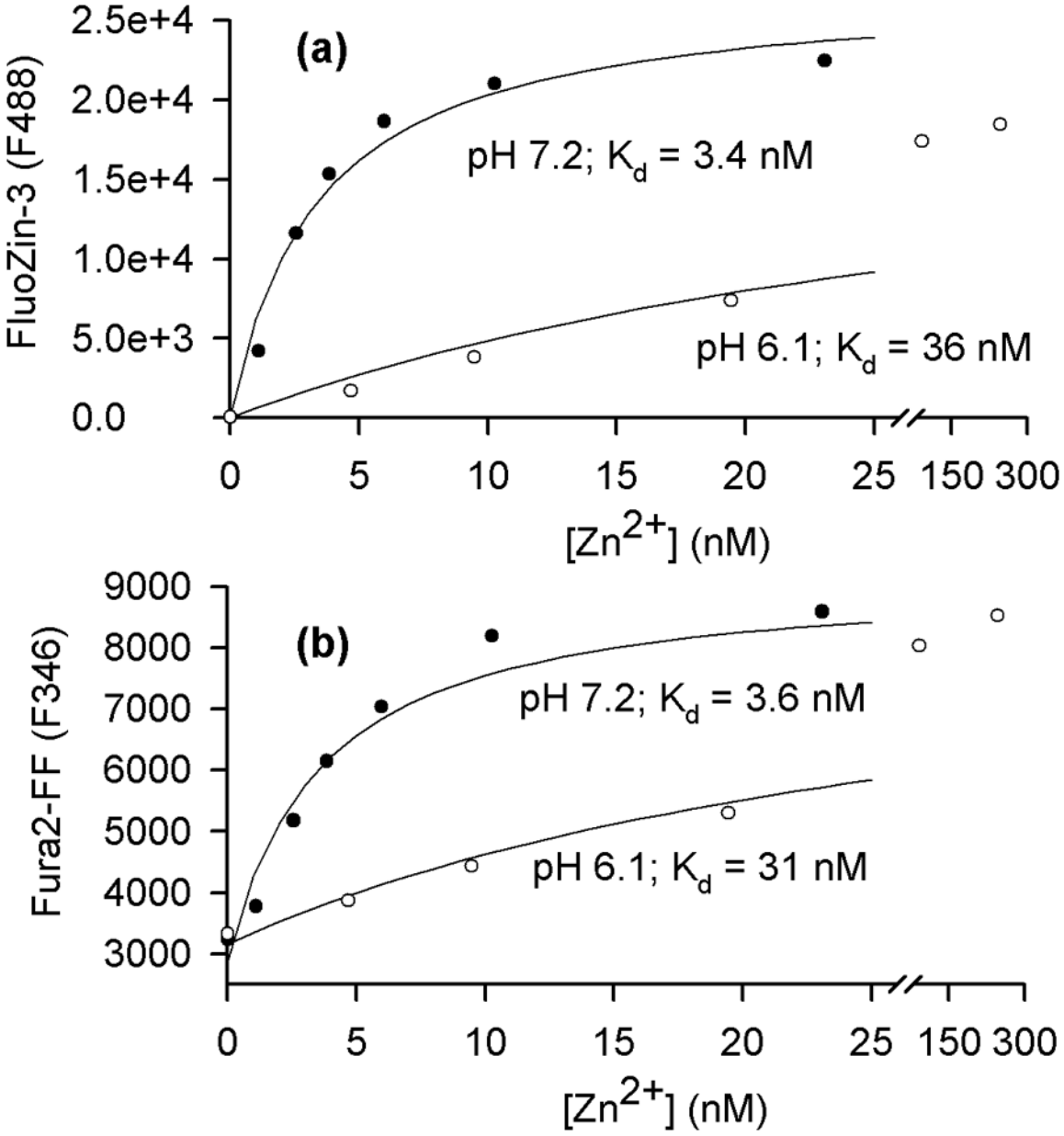

Figure 8.

A drop of pH from 7.2 to 6.1 decreases the affinity of FluoZin-3 and Fura-2FF for Zn^{2+}. (a) FluoZin-3 F488 signal was monitored *in vitro* at different [Zn^{2+}] at a pH of 7.2 and 6.1. The data were fitted as described in the Methods and yielded the indicated apparent K_d values. (b) Analogous data obtained for the Fura-2FF F346 signal.